Ultrasound in Med. & Biol., Vol. 45, No. 11, pp. 2866−2877, 2019

0301-5629/$ - see front matter

https://doi.org/10.1016/j.ultrasmedbio.2019.07.006

● *Original Contribution*

IS RADIATION-FREE ULTRASOUND ACCURATE FOR QUANTITATIVE ASSESSMENT OF SPINAL DEFORMITY IN IDIOPATHIC SCOLIOSIS (IS): A DETAILED ANALYSIS WITH EOS RADIOGRAPHY ON 952 PATIENTS

Yi-shun Wong,* Kelly Ka-lee Lai,† Yong-ping Zheng,† Lyn Lee-ning Wong,* Bobby Kin-wah Ng,* Alec Lik-hang Hung,* Benjamin Hon-kei Yip,‡ Winnie Chiu-wing Chu,§ Alex Wing-hung Ng,§ Yong Qiu,¶,‖ Jack Chun-yiu Cheng,*,‖,# and Tsz-ping Lam*,‖,#

* Department of Orthopaedics and Traumatology, The Chinese University of Hong Kong, Shatin, NT, Hong Kong SAR; † Department of Biomedical Engineering, The Hong Kong Polytechnic University, Hung Hom, Kowloon, Hong Kong; ‡ Division of Family Medicine and Primary Health Care, The Jockey Club School of Public Health and Primary Care, The Chinese University of Hong Kong, Shatin, NT, Hong Kong SAR; § Department of Imaging and Interventional Radiology, The Chinese University of Hong Kong, Shatin, NT, Hong Kong SAR; ¶ Spine Surgery, The Affiliated Drum Tower Hospital of Nanjing University Medical School, Nanjing, China; ‖ Joint Scoliosis Research Center of the Chinese University of Hong Kong and Nanjing University, Nanjing, China; and # SH Ho Scoliosis Research Laboratory, Faculty of Medicine, The Chinese University of Hong Kong, Shatin, NT, Hong Kong SAR

(*Received* 10 *March* 2019; *revised* 21 *June* 2019; *in final from* 5 *July* 2019)

Abstract—Radiation exposure with repeated radiography required at follow-up poses serious health concerns for scoliosis patients. Although spinous process angle (SPA) measurement of spinal curvatures with ultrasound has been reported with promising results, an evidence-based account on its accuracy for translational application remains undefined. This prospective study involved 952 idiopathic scoliosis patients (75.7% female, mean age 16.7 ± 3.0 y, Cobb 28.7 ± 11.6°). Among 1432 curves (88.1%) detected by ultrasound, there was good correlation between radiologic Cobb angles measured manually on EOS (E_Cobb) whole-spine radiographs and automatic ultrasound SPA measurement for upper spinal curves (USCs) (r = 0.873, apices T7−T12/L1 intervertebral disc) and lower spinal curves (LSCs) (r = 0.740, apices L1 or below) (p < 0.001). Taller stature was associated with stronger correlation. For E_Cobb <30°, 66.6% USCs and 62.4% LSCs had absolute differences between E_Cobb and predicted Cobb angle calculated from SPA ≤5°. Ultrasound could be a viable option in lieu of radiography for measuring coronal curves with apices at T7 or lower and Cobb angle <30°. (E-mail: tplam@cuhk.edu.hk)

Key Words: **Idiopathic scoliosis, Ultrasound, EOS radiography, Cobb angle, Spinous process angle.**

INTRODUCTION

Idiopathic scoliosis (IS) is a complex three-dimensional (3-D) spinal deformity in the coronal and sagittal planes with vertebral rotation in the transverse plane (Stokes et al. 1987; Hattori et al. 2011). Often diagnosed at puberty, patients are at risks of curve progression leading to significant morbidities (Cheng et al. 2015). Bracing is considered effective in preventing curve progression for immature patients (Weinstein et al. 2013; Negrini et al. 2015). Regular monitoring of scoliosis during growth is therefore important for treatment planning (Asher and Burton 2006; Weinstein et al. 2013; Cheng et al. 2015). Given that coronal Cobb angles are measured on standing posteroanterior radiographs of the whole spine taken once every 4−6 mo, repeated radiation exposure often leads to serious health concerns (Doody et al. 2000; Ronckers et al. 2010; Knott et al. 2014). Following the ALARA (As Low As Reasonably Achievable) principle of radiation safety, especially for immature patients, development of radiation-free alternatives for quantitative spinal assessment has been a long existing quest.

Being radiation-free and cost effective, ultrasound is useful for musculoskeletal imaging (Zheng et al.

Address correspondence to: Tsz-ping Lam, Department of Orthopaedics and Traumatology, The Chinese University of Hong Kong, 5/F., Clinical Science Building, Prince of Wales Hospital, Shatin, NT, Hong Kong SAR. E-mail: tplam@cuhk.edu.hk

2016; Brink et al. 2018). Compared with other imaging modalities, ultrasound is characterized by portability and dynamic scanning protocols (Zheng et al. 2016; Brink et al. 2018). Different measurement protocols on ultrasound images have been described including the center of lamina (Zheng et al. 2018; Zheng et al. 2018), spinous process angle (SPA) (Zheng et al. 2016; Zhou et al. 2017) and transverse process angle methods (Cheung et al. 2015; Brink et al. 2018). Although application of ultrasound SPA measurement for scoliosis evaluation has been reported with promising results (Table 1), relatively small cohorts of patients were investigated (Cheung et al. 2015; Li et al. 2015; Zheng et al. 2016; Zhou et al. 2017; Brink et al. 2018), and thus an evidence-based account on its accuracy under different clinical settings remains undefined. With the recent development of an algorithm for automatic SPA measurement on ultrasound images (Zhou et al. 2017), this study aimed to evaluate the reliability and validity of ultrasound for measuring coronal Cobb angle as predicted from automatic SPA measurement in IS patients with respect to different curve levels, curve severities, body mass indices, ages, genders and heights. EOS radiography was used as the gold standard.

METHODS

Patient recruitment

IS patients aged 8−40 y with body mass index (BMI) <23 kg/m^2 and standing height between 1 and 2 m were recruited at our scoliosis clinic between February 17 and December 20, 2016. Our scoliosis clinic is one of the only two tertiary referral centers for scoliosis with more than 800 new referrals received annually from the governmental scoliosis screening program for schoolchildren in Hong Kong (Lee et al. 2010; Luk et al. 2010; Fong et al. 2015). Exclusion criteria included (i) pregnancy; (ii) history of skin disease such as skin cancer or psoriasis; (iii) fracture or wound affecting ultrasound scanning; (iv) ferromagnetic implants; (v) pacemakers, pain modulators, insulin delivery systems, cochlear devices and defibrillators; (vi) previous spinal surgery; (vii) winged scapula or irregular back contour affecting ultrasound scanning; (viii) cannot stand steadily during examination; and (ix) allergy to aqueous gel for ultrasound scanning. Ethical approvals were obtained from the Institutional Review Board (Clinical Research Ethics Committee, CREC No. 2015.463). The study was registered at ClinicalTrials.gov before subject enrolment (Identifier No. NCT02581358). Written informed consents were obtained from all patients and their guardians for those below 18 y old.

EOS radiographic measurement for the spine

EOS slot-scanning radiologic system (EOS 2-D/3-D Imaging, Biospace Med, Paris, France), which is capable of simultaneous capture of standing biplanar radiographic images for the whole spine in true 1:1 scale for size and volume without magnification and distortions seen in conventional radiography, was used as the gold standard (Illés and Somoskeöy 2012). Standing posteroanterior whole-spine radiographs were taken according to standard protocols previously reported, with shoulders and elbows at 90° flexion (Hui et al. 2016; Melhem et al. 2016; Newton et al. 2016). Coronal Cobb angles (E_Cobb) of structural curves were measured manually on EOS radiographs by two independent raters blinded to ultrasound measurement (Cobb 1960). End vertebrae and apical vertebrae were identified, and “0.5” was used to indicate apex at intervertebral disc, such as T11.5 denoted T11/T12 intervertebral disc.

Ultrasound evaluation of spinal curvature with SPA measurement

Scolioscan (Telefield Medical Imaging Ltd., Hong Kong) was used for quantitative assessment of spinal curvatures (Fig. 1). Ultrasound scanning of the whole spine taken without brace were performed by two independent technicians blinded to the EOS radiographs done on the same day. Freehand scanning was done with a linear probe (10 cm width, frequency 7.5 MHz)

Table 1. Validity results of ultrasound SPA measurement reported in major pioneer studies

Authors	Journals	N (patients)	Pearson’s correlation r between Cobb angles and SPA	p value
Brink et al. 2018	*Spine Journal*	33	Thoracic ≥ 0.993 Lumbar ≥ 0.985	Not given
Zhou et al. 2017	*IEEE Transactions on Medical Imaging*	29	0.830	<0.001
Zheng et al. 2016	*Scoliosis and Spinal Disorders*	49	Thoracic ≥ 0.883 Lumbar ≥ 0.849	Not given
Li et al. 2015	*Spine Deformity*	33	0.792	<0.05
Cheung et al. 2015	*IEEE Transactions on Medical Imaging*	29	0.889	<0.001

SPA = spinous process angle.

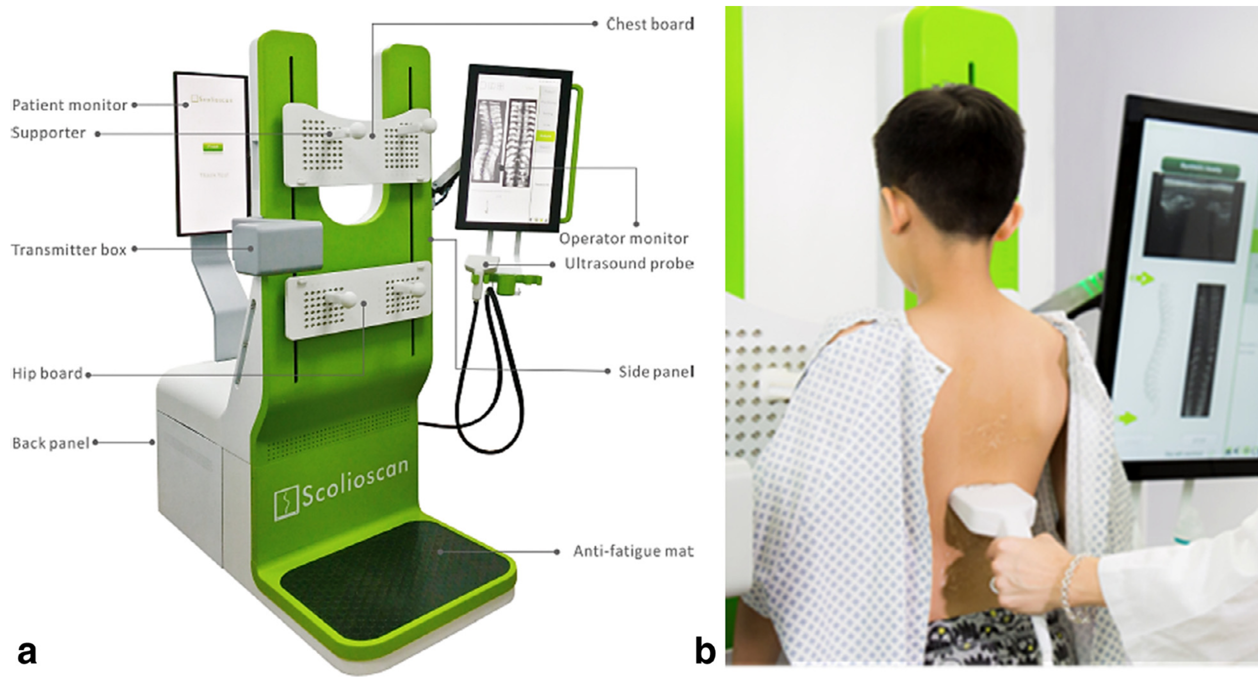

Fig. 1. (a) The Scolioscan system with its components labeled. The ultrasound scanner, computer and spatial sensor control box were installed inside the device. (b) Ultrasound assessment for a patient.

equipped with an electromagnetic spatial sensing device (Cheung et al. 2013; Zheng et al. 2016).

Given that ultrasound setting may affect image quality, thus affecting identification of bony landmarks and subsequent measurement of angles, trials on a large number of patients have been conducted earlier to obtain optimal ultrasound setting which suits for most cases. Using the default setting of depth (7.1 cm), focus (3.5 units), frequency (7.5 MHz), brightness (34 db) and contrast (118 db), high-quality ultrasound images could be obtained for most cases. For a specific case, if the default setting could not provide high-quality images, operators would adjust the setting to optimize image quality. The criterion for the adjustment was to have bony features clearly visualized.

Concerning calibration of the Scolioscan system, the 3-D spatial information of the probe was determined using an electromagnetic sensing method, which had a transmitter installed in the machine and a sensor installed inside the ultrasound probe. The spatial sensing was pre-calibrated by the manufacturer during installation to make sure the spatial data were accurately measured and not affected by any error sources, such as nearby big metal structures. Daily calibration by operators was done to ensure there was no undesired movement of the spatial sensing element, as well as no interference from any nearby installed devices surrounding the system. The calibration procedure was performed by using the ultrasound probe to scan over a long, straight wooden block vertically fixed at the location for subject standing. If the coronal image formed was not straight, interference or other error sources could be present. According to the manufacturer, if curvature of greater than one degree was detected, the source of error should be determined for rectification. In our study, such case was very rare.

For the ultrasound assessment, after undressing the upper garments and shoes, the patient was requested to stand on the Scolioscan platform facing the supporting boards for supporters' adjustment. The chest and hip boards were repositioned according to the patient's height. Two supporters on the chest board were relocated to align with the clavicle anterior concavities, whereas two supporters on the hip board were relocated to align with the bilateral anterior superior iliac spine. The length of supporter's shafts on both boards was adjusted until they were just in touch with the patient. By keeping in light contact with the positional posts, these supporters were used to help patient maintain a stable natural standing posture when minimal pressure was exerted from the ultrasound probe for minimization of body displacement during the ultrasound scanning. The patient was instructed to maintain a natural standing posture with shallow breathing after adjustment of the supporters and to keep his/her eye level horizontal to the eye spot shown on the screen in front of them throughout the scanning process. Adequate amount of ultrasound gel was applied onto the patient to fill all gaps between the probe and patient's skin so as to assure ultrasound image quality. Spinal column was scanned steadily from L5 up to T1 vertebra. The

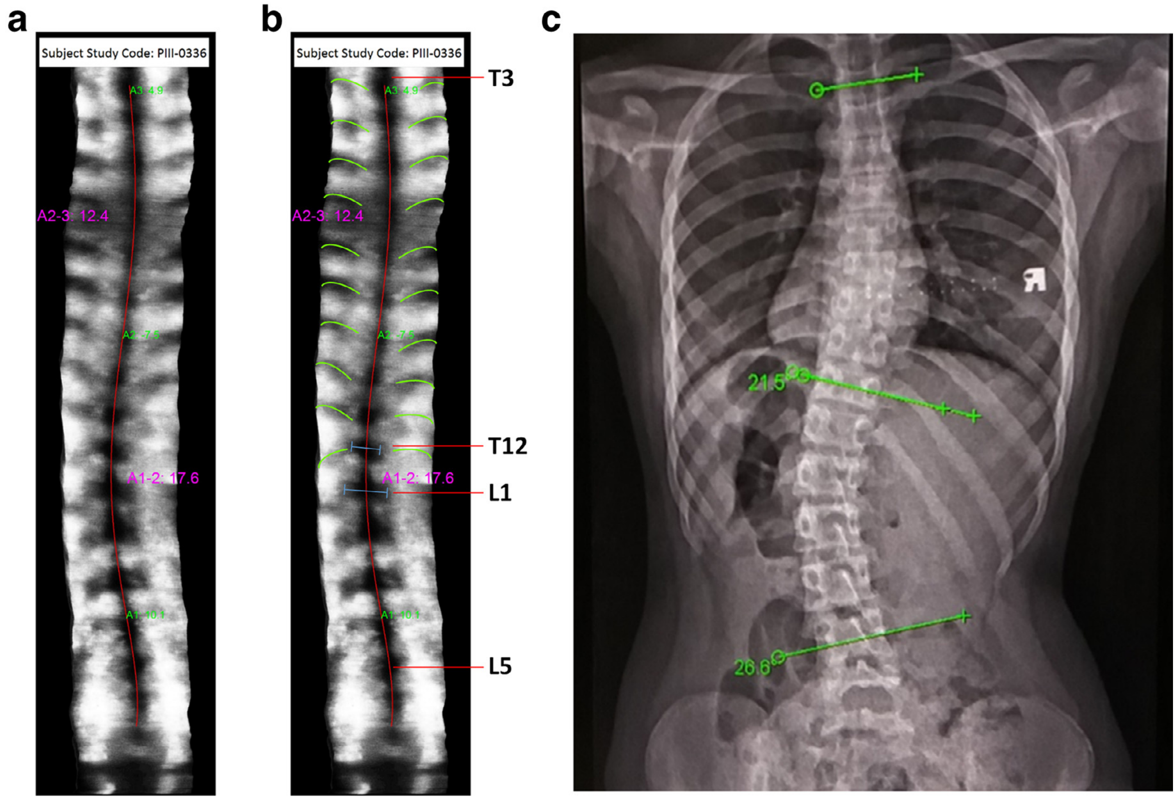

Fig. 2. (a) An ultrasound volume projection image of the spine showing line of spinous processes (indicated by red line) with which SPAs were measured automatically. SPA for curve between A1 and A2 is denoted as A1-2 = 17.6˚. SPA for curve between A2 and A3 is denoted as A2-3 = 12.4˚. (b) T3, T12, L1 and L5 vertebrae are indicated in the ultrasound image. T12 vertebra can be identified due to the appearance of the rib (indicated by green lines) as well as the significant difference of the width (indicated by blue lines) of the vertebra visualized in the coronal ultrasound image between T12 (being narrower) and L1 (being wider). (c) Corresponding EOS posteroanterior image of the spine for the same subject. SPA = spinous process angle.

scanning took approximately 30−60 s, depending on the height of the patient.

Two-dimensional B-mode images and spatial orientation data were incorporated to construct volume projection images for the whole spine (Cheung et al. 2015; Zhou et al. 2017). In-built computer program was used to determine the best-fitting curvilinear line passing through the spinous processes with which the SPAs were automatically measured (Zhou et al. 2017) (Fig. 2). The working principles of the software for automatic measurement of spinal curvatures have been reported (Zhou et al. 2017). The central black profile was first automatically detected; a six-order polynomial curve was then used to fit all the detected profile. The turning points were automatically identified from which the angle between two neighboring points was calculated (Zhou et al. 2017). Approximately 10−30 s were required for data processing, and the whole ultrasound assessment process including data entry and patient positioning took around 5−10 min, which was comparable to that for EOS radiographic assessment.

Demographic and anthropometric measurement

Weight and height were measured. Corrected height to adjust for scoliosis was calculated with the Bjure formula (Bjure et al. 1968). Corrected BMI was calculated as weight/corrected height^2 (kg/m^2).

Statistical analysis

Intra-class correlation was used to evaluate inter and intra-observer reliability. Validity of ultrasound measurement under various clinical parameters was evaluated with linear regression, with E_Cobb being the dependent variables and SPA being the independent variable. Conversion formulae were developed to predict E_Cobb by calculating the predicted Cobb angle (P_Cobb) as a function of SPA. To test the agreement between E_Cobb and P_Cobb, the difference between P_Cobb and E_Cobb was analyzed both with cross tabulation and Bland-Altman plots. All analyses were performed using SPSS version 24.0 (IBM Corp., Armonk, NY, USA). The level of significance was set at 0.05.

Sample size estimation

Curves were categorized into 10 subgroups according to the apical levels from T6 to L3. Assuming a modest correlation of 0.4, type I error of 0.01 (two sided) and power of 95%, 102 curves were required for each subgroup according to the sample size calculator available at the Centre for Clinical Research and Biostatistics, The Chinese University of Hong Kong. Since there were 10 subgroups, 1000 patients with one or more structural curves were recruited. Curve severity was categorized into two subgroups, namely E_Cobb <30° and ≥30°; BMI, ages and heights were analyzed according to quartiles subgroups. At the end of the study, 952 patients with 1432 matched curves were available and considered adequate for analysis.

RESULTS

Of 1970 consecutive eligible patients, 48 were excluded because of absence of any structural curves (E_Cobb <10°). A total of 952 IS patients (721 females and 231 males, mean age 16.7 ± 3.0 y) were finally enrolled into the study (Fig. 3). Demographic and anthropometric data were shown in Table 2.

The intra- and inter-observer reliability using intraclass coefficient (ICC) (2, 1) were 0.988 and 0.949 for E_Cobb measurement; 0.916 and 0.838 for automatic ultrasound SPA measurement, respectively. A total of 1625 coronal structural curves (mean E_Cobb 28.7 ± 11.6°, range 10.1−86.7°) were identified on EOS radiographs, of which (i) 1432 curves (88.1%) were detected by ultrasound (E_Cobb 29.3 ± 11.8°; SPA 18.4 ± 8.5°), (ii) three curves (0.2%) had mismatch of curve direction (E_Cobb 18.2 ± 2.8°; SPA 8.8 ± 1.5°) and (iii) 190 curves (11.7%) were not detected by ultrasound (E_Cobb 24.2 ± 9.2°). In addition, 357 redundant curves were recorded by ultrasound (SPA 11.6 ± 6.0°) that were considered non-structural on EOS radiographs (E_Cobb <10° or end-vertebra tilt angles <5°).

Among the 1432 radiographic curves detected by ultrasound, significant correlation was noted between E_Cobb and SPA, with an overall Pearson's correlation

Table 2. Demographic characteristics of the 952 IS patients (721 females and 231 males)

Parameters	Mean ± SD	Range
Age (y)	16.7 ± 3.0	9.3−31.4
Weight (kg)	48.5 ± 7.5	25.3−74.4
Corrected body height (cm)	163.0 ± 8.3	135.0−188.6
Corrected body mass index (kg/m^2)	18.2 ± 1.9	13.0−22.7

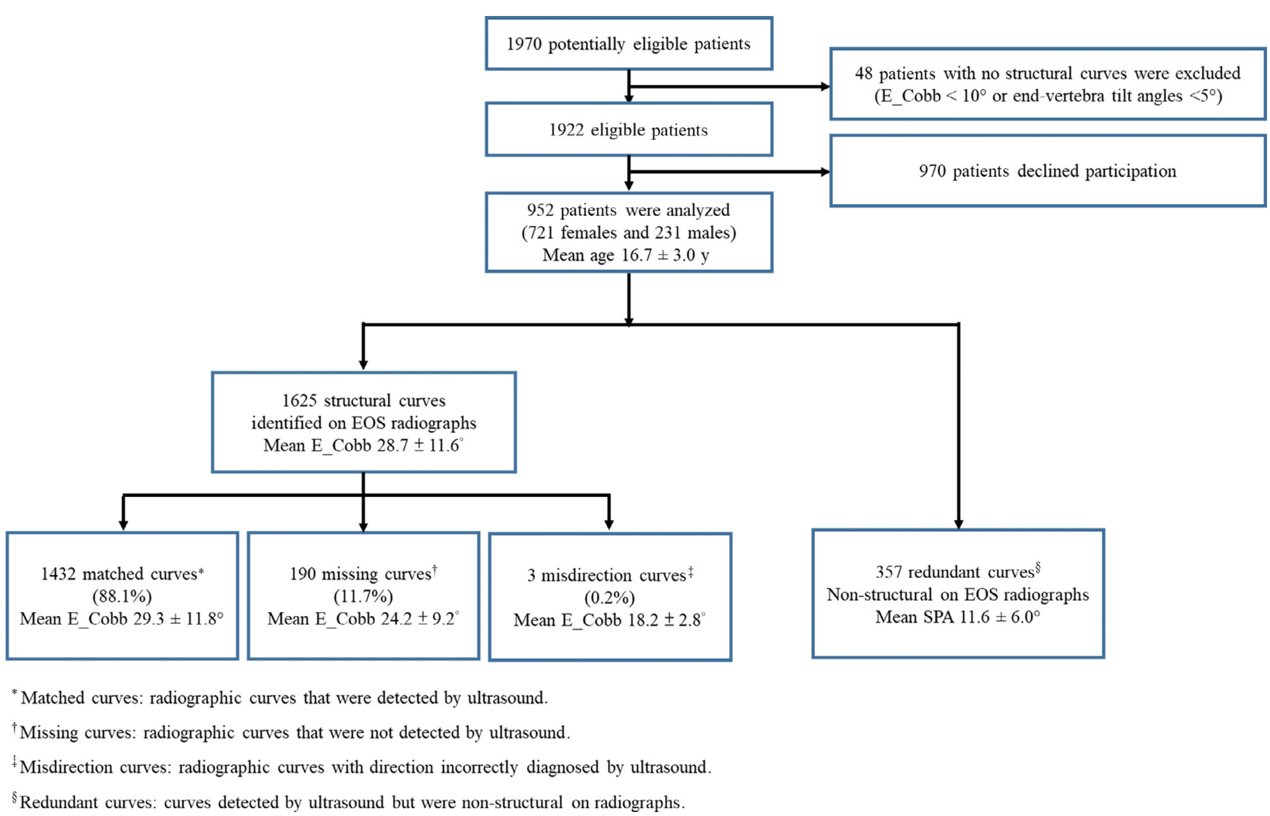

Fig. 3. Study flow diagram.

Table 3. Correlation between E_Cobb and SPA at different curve levels

EOS apex	N (number of curves)	Pearson's correlation r	p value
T3-T3.5	14	0.239	0.410
T4-T4.5	9	0.807	0.009*
T5-T5.5	16	0.408	0.116
T6-T6.5	61	0.703	<0.001†
T7-T7.5	160	0.872	<0.001†
T8-T8.5	258	0.887	<0.001†
T9-T9.5	152	0.888	<0.001†
T10-T10.5	73	0.840	<0.001†
T11-T11.5	44	0.825	<0.001†
T12-T12.5	71	0.818	<0.001†
L1-L1.5	193	0.692	<0.001†
L2-L2.5	303	0.788	<0.001†
L3-L3.5	75	0.705	<0.001†
L4	3	0.803	0.407

Note. End vertebrae and apical vertebrae were identified, and "0.5" was used to indicate apex at intervertebral disc, such as T11.5 denoted T11/T12 intervertebral disc.

E_Cobb = Cobb angle measured manually on EOS; SPA = spinous process angle.

* $p < 0.05$.

† $p < 0.01$.

coefficient (r) of 0.816 ($p < 0.001$). Correlation results with respect to curve apices from T3 down to L4 were shown in Table 3. Based on the correlation strength with cutoff threshold set at 0.8, curves were classified into (i) upper thoracic curves (UTCs) (apices at T6.5 or above, n = 100, $r = 0.629$); (ii) upper spinal curves (USCs) (apices between T7 and T12/L1 intervertebral disc (T12.5), n = 758, $r = 0.873$); and (iii) lower spinal curves (LSCs) (apices at L1 or below, n = 574, $r = 0.740$), all with $p < 0.001$. Scatterplots between E_Cobb and SPA for all structural curves, UTCs, USCs and LSCs are shown in Figure 4. Conversion formulae to predict Cobb angle (designated as P_Cobb) from SPA were developed for USC: [P_Cobb = 7.39 + 1.26 × SPA] and LSC: [P_Cobb = 10.08 + 0.96 × SPA]. The difference of P_Cobb minus E_Cobb in relation to E_Cobb subgroups is tabulated in Table 4. For curves with E_Cobb <30°, 66.6% USCs and 62.4% LSCs had absolute difference between E_Cobb and P_Cobb ≤5°, whereas P_Cobb underestimated E_Cobb by >5° in 6.0% of USCs and 7.2% of LSCs, respectively. Bland-Altman plots for USC and LSC are displayed in Figure 5.

Correlation with respect to subgroups of genders, BMI, heights and ages is shown in Table 5. Correlation between E_Cobb and SPA was numerically stronger for taller statures and greater ages, whereas correlation strength was similar between genders or different quartiles of BMI.

Among the 190 radiologic curves (11.7%) that were not detected by ultrasound, 60 were the major curves for the affected patients while 130 were non-major curves. The distribution with respect to curve levels and end-vertebra tilt angles is shown in Table 6.

Among 1000 patients who underwent ultrasound scanning, six patients (0.6%) felt dizzy during the procedure. After taking some rest, all patients fully recovered with no residual sequelae.

DISCUSSION

Overall, the reliability of automatic ultrasound SPA measurement was excellent (ICC > 0.8). So was the validity as evaluated with Pearson correlation ($r = 0.816$) between E_Cobb measured with radiography and SPA with ultrasound scanning. These results were consistent with previous studies based on 33 and 49 patients, respectively, by Zheng et al. (2016) and Brink et al. (2018) reporting inter-rater reliability of ultrasound SPA measurements ranging from 0.86−0.95 and correlation between ultrasound SPA and radiologic Cobb angles ranging from 0.85−0.99. With a larger sample size and detailed subgroup analyses, this study provided further clinical information on relationship between validity of ultrasound measurement and curve apical levels, curve severity and other clinical parameters.

Concerning apical levels, the best correlation between ultrasound and radiographic measurements was observed for the USCs with apices between T7 and T12.5, whereas moderate but still significant correlation was noted for the LSCs with apices at L1 or below. In contrast, weak correlation of 0.629 was seen for UTCs with apices at T6.5 or above. The lower correlation observed for UTC could be attributed to scapular prominence that interferes with scanning movement of the ultrasound probe (Zheng et al. 2016; Brink et al. 2018). This is especially true when the standard probe with a width of 10 cm is negotiated between both scapulae. Awareness of this technical difficulty and careful manipulation of the probe between the scapulae should be exercised in order to obtain the best ultrasound images. In addition, upper thoracic vertebrae are more crowded, thus affecting the quality of ultrasound measurement (Lou et al. 2015; Zheng et al. 2016; Brink et al. 2018).

Unlike previous findings by Zheng et al. (2016) and Brink et al. (2018) who reported similar validity of ultrasound measurement for thoracic curves (defined as apices at T11.5 or above) and lumbar curves (apices at T12 or below), this study showed that correlation was numerically greater for USC (apices T7 to T12.5) than LSC (apices L1 or lower). Coronal ultrasound measurements focus on spinous processes that are located more posterior than vertebral bodies on which radiographic Cobb angles are measured, thus leading to different curve projection (Zheng et al. 2016; Brink et al. 2018). As a result of apical vertebral rotation toward the concavity, raw

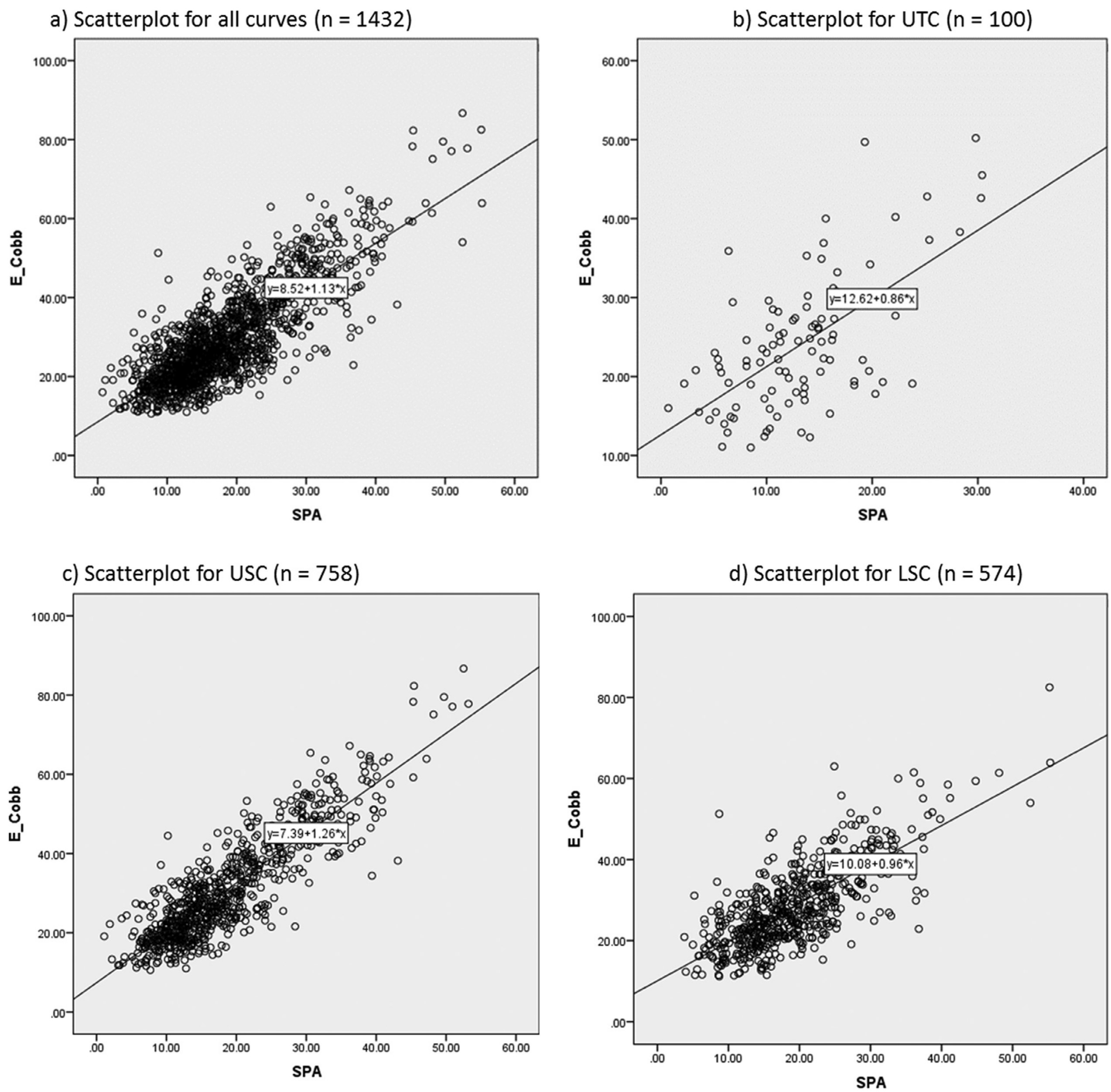

Fig. 4. Scatterplot between E_Cobb and SPA. E_Cobb = Cobb angle measured manually on EOS; SPA = spinous process angle; UTC = upper thoracic curve; USC = upper spinal curve; LSC = lower spinal curve.

SPA measurements are usually numerically lower than radiologic Cobb measurements (Zheng et al. 2016; Brink et al. 2018). Our result was consistent with this observation in that the mean E_Cobb was 29.3 ± 11.8° compared with 18.4 ± 8.5° for SPA. Morrison et al. (2015) reported addition of apical vertebral rotation parameter improved prediction of the Cobb angle by ultrasound. With further development of ultrasound technology for measuring vertebral axial rotation to be incorporated into the prediction model, it is possible that the accuracy of ultrasound measurement can be further improved especially for LSC.

Table 4. Cross tabulation of curve severity (E_Cobb) against the difference of P_Cobb minus E_Cobb

	E_Cobb (°)	N (curves)	Range of difference (°)*	Overestimation > +5.0°	Desirable +5.0° to −5.0°	Underestimation < −5.0°
			USC (n = 758), *P*_Cobb = 7.39 + 1.26 × SPA			
	<30.0	434	−13.0 to +21.6	27.4%	66.6%	6.0%
	≥30.0	324	−24.3 to +23.5	9.3%	53.4%	37.3%
Overall	10.6−86.7	758	−24.3 to +23.5	19.7%	60.9%	19.4%
			LSC (n = 574), *P*_Cobb = 10.08 + 0.96 × SPA			
	<30.0	362	−10.4 to +22.5	30.4%	62.4%	7.2%
	≥30.0	212	−32.9 to +14.5	4.7%	49.5%	45.8%
Overall	11.2−82.5	574	−32.9 to +22.5	20.9%	57.7%	21.4%

Note. USCs with apices between T7 and T12.5. LSCs with apices at L1 or below.
E_Cobb = Cobb angle measured manually on EOS; P_Cobb = predicted Cobb angles; USC = upper spinal curve; SPA = spinous process angle; LSC = lower spinal curve.
* Difference between P_Cobb and E_Cobb = P_Cobb minus E_Cobb. Positive values indicated P_Cobb overestimated E_Cobb.

Apart from curve levels, curve severity also affected accuracy of ultrasound measurement. In the present study, good agreement was seen between EOS and ultrasound measurement when E_Cobb was below 30°. About 66.6% of USCs and 62.4% of LSCs had absolute difference between E_Cobb and P_Cobb within the clinical acceptable margin of 5°, whereas only 6.0% of USCs and 7.2% of LSCs had curve severity underestimation of >5° by P_Cobb (Gross et al. 1983; Carman et al. 1990). As shown in Table 4 and Figure 5, accuracy of ultrasound measurement was lower when E_Cobb was ≥30°. Morrison et al. (2015) reported that greater curve severity was associated with greater vertebral rotation. Zheng et al. (2018) also reported large axial vertebral rotation that normally occurred in curves with larger Cobb angles, thus presenting a higher percentile of large discrepancy curves with Cobb angle ≥25° than the mild curves (7% vs. 3%). For improvement of ultrasound measurement, inclusion of apical vertebral rotation into the prediction model would be desirable especially for Cobb ≥30°.

Although radiography is still required for (i) diagnosis of IS by ruling out underlying abnormalities at the first visit, (ii) treatment decision for bracing or surgery and (iii) patients with previous surgery or metal implants, the satisfactory validation of ultrasound for Cobb <30° justified its use in lieu of radiography to reduce unnecessary radiation exposure especially for

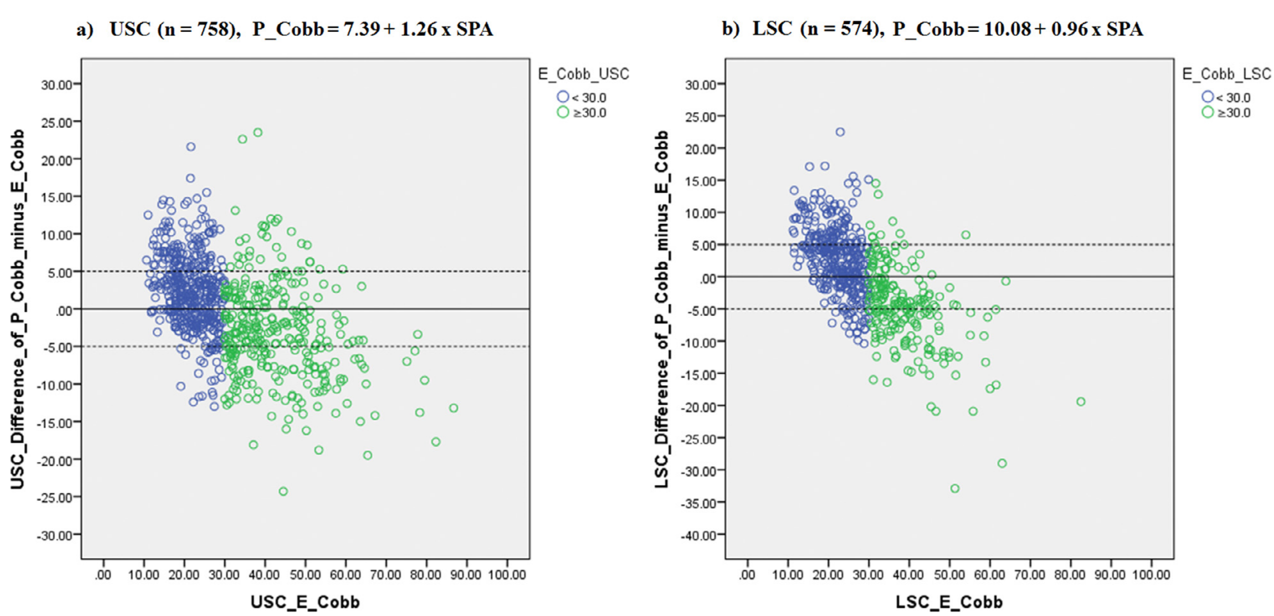

Fig. 5. Bland-Altman plot of curve severity (E_Cobb) against the difference of P_Cobb minus E_Cobb. E_Cobb = Cobb angle measured manually on EOS; P_Cobb = predicted Cobb angle; USC = upper spinal curve; LSC = lower spinal curve.

Table 5. Correlation between E_Cobb and SPA under different clinical parameters

Parameters	Grouping	Median	Range	N (curves)	Pearson's correlation r	p value
Gender	Female	-	-	1104	0.815	<0.001
	Male	-	-	328	0.813	<0.001
Age	First quartile	13.7	9.3−14.8	358	0.769	<0.001
	Second quartile	15.5	14.8−16.3	358	0.752	<0.001
	Third quartile	17.2	16.3−18.2	358	0.827	<0.001
	Fourth quartile	19.7	18.2−31.4	358	0.849	<0.001
Corrected BMI	First quartile	16.0	13.0−16.8	358	0.835	<0.001
	Second quartile	17.5	16.8−18.1	358	0.783	<0.001
	Third quartile	18.8	18.1−19.4	358	0.819	<0.001
	Fourth quartile	20.5	19.4−22.7	358	0.820	<0.001
Corrected body height	First quartile	154.4	135.0−157.3	358	0.760	<0.001
	Second quartile	159.6	157.3−162.1	358	0.805	<0.001
	Third quartile	164.9	162.1−167.9	358	0.825	<0.001
	Fourth quartile	172.3	167.9−188.6	358	0.860	<0.001

E_Cobb = Cobb angle measured manually on EOS; SPA = spinous process angle; BMI = body mass index.

immature patients requiring regular follow-up for mild and early scoliosis. It has been proposed that ultrasound could be considered for community scoliosis screening (Letts et al. 1988; Mauritzson et al. 1991; Cheung et al. 2015; Zheng et al. 2016) and detection of curve progression (Zheng et al. 2018). Our findings revealed that ultrasound is accurate for curves with Cobb angle <30°, which supports the use of ultrasound for scoliosis screening. In this regard, further clinical studies evaluating the accuracy of ultrasound for scoliosis screening are warranted. On the other hand, ultrasound could be considered an alternative to radiography for monitoring of curve progression during subsequent follow-up so as to reduce X-ray exposure but keeping in mind that confirmatory radiography should be considered whenever curve progression is detected with ultrasound measurements.

Table 6. Frequency distribution of radiologic curves that were not detected by ultrasound (total n = 190)

Distribution	UTC	Non-UTC	Total
The missed radiologic curve was the major curve for the patient (n = 60)			
Either end-vertebral tilt angles <10°	26 (43.3%)	11 (18.3%)	37 (61.7%)
Both end-vertebral tilt angles ≥10°	21 (35.0%)	2 (3.3%)	23 (38.3%)
Total	47 (78.3%)	13 (21.7%)	60 (100%)
The missed radiologic curve was not the major curve for the patient (n = 130)			
Either end-vertebral tilt angles <10°	82 (63.1%)	22 (16.9%)	104 (80.0%)
Both end-vertebral tilt angles ≥10°	22 (16.9%)	4 (3.1%)	26 (20.0%)
Total	104 (80.0%)	26 (20.0%)	130 (100%)

Note. UTCs with apices at T6.5 or above; non-UTCs with apices at T7 or below.

UTC = upper thoracic curve; non-UTC = non-upper thoracic curve.

It is noteworthy that 19.7% of USC and 20.9% of LSC had curve severity overestimated of >5° by ultrasound. For clinical management, curve overestimation is of less concern than underestimation, because overestimation will prompt investigation with radiography for treatment planning (Zheng et al. 2018). The purpose of measuring spinal curvatures with ultrasound is not to replace radiography completely, but to avoid radiography as far as reasonably practicable (Brink et al. 2018; Zheng et al. 2018).

Another interesting finding from this study was that numerically stronger correlation was seen with patients of taller stature and greater age. Height may play an important role on validity of ultrasound measurement. Increased height corresponds to longer spinal length, which is more accessible to ultrasound scanning. In this regard, multicenter studies investigating different ethnic groups are warranted to evaluate the impacts of height and other ethnic-related factors on accuracy of ultrasound measurement.

The detection rate of major structural curves by the current ultrasound system was 93.7%. Among the 60 major curves that were missed, 47 (78.3%) were UTCs and 37 (61.7%) had end-vertebra tilt angles <10°. These were consistent with results reported by Lou et al. (2015), who mentioned that only 80% of curves were recognized by ultrasound but with 95% of major curves being detected while most ultrasound missing curves were either non-structural or UTCs. A detailed comparison of EOS and ultrasound images showed that further improvement of the algorithm of in-built automatic SPA measurement to detect more than two curves will likely reduce the missing rate by ultrasound (Fig. 6).

Although this study shows that ultrasound is satisfactory for quantitative measurement of spinal

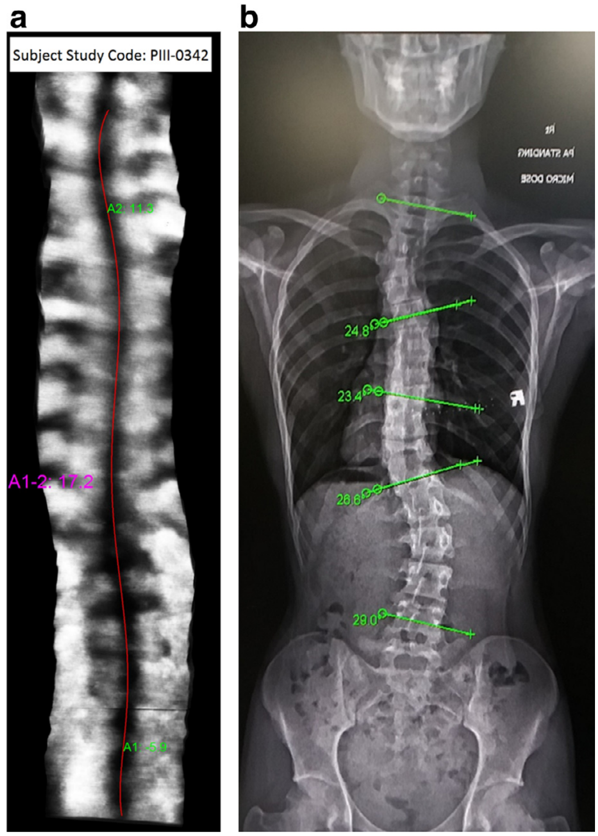

Fig. 6. An example illustrating the Scolioscan missing curves, (a) ultrasound image and (b) corresponding EOS image.

deformity, it is speculated that improvement in the following aspects could further enhance the applicability of ultrasound for scoliosis evaluation. First, extending the scanning region to include the lower cervical region may improve measurement for UTCs. Second, because scapulae would disturb ultrasound probe movement during scanning, a smaller probe or the possibility to move the probe obliquely can be considered. Third, vertebral axial rotation characterizes IS (Ungi et al. 2014; Zheng et al. 2016). The presence of significant deviation of the spinous processes due to vertebral lateral deviation, intrinsic axial rotational and torsional deformity of scoliotic vertebrae might affect the accurate interpretation of the vertebral body alignment and the angle measurement on the ultrasound images (Fig. 7) (Ungi et al. 2014; Zheng et al. 2016). In this study, conversion formulae developed to predict E_Cobb were simple linear equation based on 758 and 574 curves, with moderate to good correlation of 0.873 and 0.740, respectively, for USC and LSC. By incorporating rotation parameters, correlation between E_Cobb and SPA can be further improved especially for LSCs. Fourth, although dizziness is not common (0.6%), it is worthwhile to adopt relaxing environment in the ultrasound suite with good ventilation, reduced overhead light sources and brightness of monitor facing the patients. An assistant should always be available to provide assistance during scanning in case patients feel dizzy during the procedure.

There are limitations with this study. First, although IS patients aged 8−40 were recruited, the mean age of the patients studied were 16.7 ± 3.0 y near skeletal maturity (Cheng et al. 2015). As mentioned before, correlation coefficients between E_Cobb and SPA were numerically greater with taller statures and greater ages. Accuracy of ultrasound measurement for patients aged around 10, especially for females with years since menarche less than 2 y who are prone to curve progression deserves our focus for further investigation (Cheng et al. 2015; Brink et al. 2018). Second, this study only recruited Chinese patients. Future studies including different ethnic groups are warranted. Third, sagittal and rotational parameters in the transverse plane were not investigated. For complete evaluation of spinal deformity, 3-D assessment will be desirable.

CONCLUSIONS

The accuracy of ultrasound automatic SPA measurement under the clinical parameters of curve levels, curve severities, body mass indices, ages, genders and heights has been evaluated in the present large-scale clinical study. Conventional radiography is still required for the first clinical assessment for scoliosis patients to rule out underlying bony anomalies. For subsequent follow-up evaluation, ultrasound can be a viable alternative to radiography for radiation-free evaluation of curves with apices at T7 or below and Cobb angles $<30^\circ$ especially for immature patients with mild and early scoliosis requiring regular long-term follow-up till skeletal maturity. For curves $\geq 30^\circ$, or with apices at T6.5 or above, conventional radiography is preferred.

Acknowledgments—The authors thank the contribution of Yen Siu-yin Law, Fiona Wai Ping Yu, Echo Ka Ling Tsang and Josephine Wing Lam Yau for their assistance in conducting the study.

The study was investigator-initiated. Our department at The Chinese University of Hong Kong received an unconditional donation for supporting scoliosis-related research and education from Telefield Medical Imaging Ltd. The donor was not involved in data collection, analysis, interpretation and the decision for publication. The corresponding author had full access to all data and the final responsibility for submission and publication.

Conflict of interest disclosure—YPZ was an inventor of a number of patents related to the Scolioscan system, which have been licensed to Telefield Medical Imaging Limited through the Hong Kong Polytechnic University. YPZ also served as the consultant to Telefield Medical Imaging Limited to improve the function of the Scolioscan system. TPL's institute Department of Orthopaedics and Traumatology of the Chinese University of Hong Kong received an unconditional donation for supporting scoliosis-related research and education from Telefield Medical Imaging Ltd. All other authors declare no conflict of interest. The study

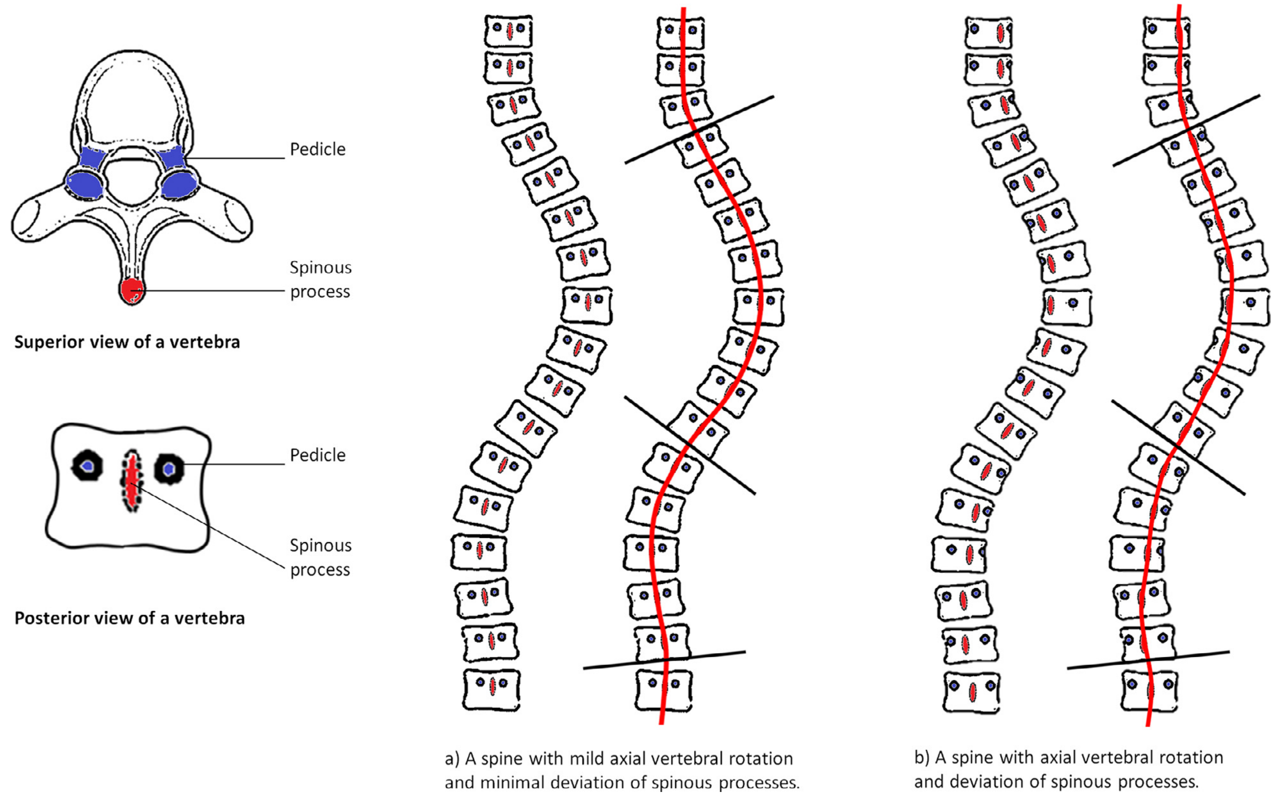

Fig. 7. Illustration of the potential problem of spinous process deviation due to axial vertebral rotation that may affect the accuracy of ultrasound SPA measurement. The lines of spinous processes (red lines) indicate that SPA would underestimate the degree of a spinal curve when spinous process deviation due to axial vertebral rotation is present (b), compared with (a), where axial vertebral rotation is mild and the SPA better estimates the degree of a spinal curve. SPA = spinous process angle.

was an investigator-initiated study. The donor was not involved in the collection, analysis, interpretation of the data and the decision to approve publication of the finished manuscript. The corresponding author had full access to all the data in the study and had final responsibility for the decision to submit for publication.

REFERENCES

Asher MA, Burton DC. Adolescent idiopathic scoliosis: Natural history and long term treatment effects. Scoliosis 2006;1:2.

Bjure J, Grimby G, Nachemson A. Correction of body height in predicting spirometric values in scoliotic patients. Scand J Clin Lab Invest 1968;21:191–192.

Brink RC, Wijdicks SPJ, Tromp IN, Schlösser TPC, Kruyt MC, Beek FJA, Castelein RM. A reliability and validity study for different coronal angles using ultrasound imaging in adolescent idiopathic scoliosis. Spine J 2018;18:979–985.

Carman DL, Browne RH, Birch JG. Measurement of scoliosis and kyphosis radiographs. Intraobserver and interobserver variation. J Bone Joint Surg Am 1990;72:328–333.

Cheng JC, Castelein RM, Chu WC, Danielsson AJ, Dobbs MB, Grivas TB, Gurnett CA, Luk KD, Moreau A, Newton PO, Stokes IA, Weinstein SL, Burwell RG. Adolescent idiopathic scoliosis. Nat Rev Dis Primers 2015;1:15030.

Cheung CW, Law SY, Zheng YP. Development of 3-D ultrasound system for assessment of adolescent idiopathic scoliosis (AIS): And system validation. Conf Proc IEEE Eng Med Biol Soc 2013;2013:6474–6477.

Cheung CW, Zhou GQ, Law SY, Mak TM, Lai KL, Zheng YP. Ultrasound volume projection imaging for assessment of scoliosis. IEEE Trans Med Imaging 2015;34:1760–1768.

Cobb J. The problem of the primary curve. J Bone Joint Surg Am 1960;42:1413–1425.

Doody MM, Lonstein JE, Stovall M, Hacker DG, Luckyanov N, Land CE. Breast cancer mortality after diagnostic radiography: Findings from the U.S. Scoliosis Cohort Study. Spine (Phila Pa 1976) 2000;25:2052–2063.

Fong DY, Cheung KM, Wong YW, Wan YY, Lee CF, Lam TP, Cheng JC, Ng BK, Luk KD. A population-based cohort study of 394,401 children followed for 10 years exhibits sustained effectiveness of scoliosis screening. Spine J 2015;15:825–833.

Gross C, Gross M, Kuschner S. Error analysis of scoliosis curvature measurement. Bull Hosp Jt Dis Orthop Inst 1983;43:171–177.

Hattori T, Sakaura H, Iwasaki M, Nagamoto Y, Yoshikawa H, Sugamoto K. In vivo three-dimensional segmental analysis of adolescent idiopathic scoliosis. Eur Spine J 2011;20:1745–1750.

Hui S, Pialasse J, Wong J, Lam T, Ng B, Cheng J, Chu W. Radiation dose of digital radiography (DR) versus micro-dose x-ray (EOS) on patients with adolescent idiopathic scoliosis: 2016 SOSORT-IRSSD "John Sevastic Award" winner in imaging research. Scoliosis Spinal Disord 2016;11:46.

Illés T, Somoskeöy S. The EOS imaging system and its uses in daily orthopaedic practice. Int Orthop 2012;36:1325–1331.

Knott P, Pappo E, Cameron M, Demauroy J, Rivard C, Kotwicki T, Zaina F, Wynne J, Stikeleather L, Bettany-Saltikov J, Grivas TB, Durmala J, Maruyama T, Negrini S, O'Brien JP, Rigo M. SOSORT 2012 consensus paper: Reducing x-ray exposure in pediatric patients with scoliosis. Scoliosis 2014;9:4.

Lee C, Fong D, Cheung K, Cheng J, Ng B, Lam T, Mak K, Yip P, Luk K. Referral criteria for school scoliosis screening: Assessment and recommendations based on a large longitudinally followed cohort. Spine (Phila Pa 1976) 2010;35:E1492–E1498.

Letts M, Quanbury A, Gouw G, Kolsun W, Letts E. Computerized ultrasonic digitization in the measurement of spinal curvature. Spine 1988;13:1106–1110.

Li M, Cheng J, Ying M, Ng B, Lam TP, Wong MS. A preliminary study of estimation of Cobb's angle from the spinous process angle using a clinical ultrasound method. Spine Deform 2015;3:476–482.

Lou E, Zheng R, Chan AC, Hill DL, Moreau MJ, Hedden DM, Mahood JK, Southon S. Reliability of coronal curvature measurements on 3 D ultrasound images for AIS. Scoliosis 2015;10:O37.

Luk K, Lee CF, Cheung K, Cheng J, Ng B, Lam T, Mak K, Yip P, Fong D. Clinical effectiveness of school screening for adolescent idiopathic scoliosis: A large population-based retrospective cohort study. Spine (Phila Pa 1976) 2010;35:1607–1614.

Mauritzson L, Ilver J, Benoni G, Lindstrom K, Willner S. Two-dimensional airborne ultrasound real-time linear array scanner - Applied to screening for scoliosis. Ultrasound Med Biol 1991;17:519–528.

Melhem E, Assi A, El Rachkidi R, Ghanem I. EOS(®) biplanar X-ray imaging: Concept, developments, benefits, and limitations. J Child Orthop 2016;10:1–14.

Morrison DG, Chan A, Hill D, Parent EC, Lou EH. Correlation between Cobb angle, spinous process angle (SPA) and apical vertebrae rotation (AVR) on posteroanterior radiographs in adolescent idiopathic scoliosis (AIS). Eur Spine J 2015;24:306–312.

Negrini S, Minozzi S, Bettany-Saltikov J, Chockalingam N, Grivas TB, Kotwicki T, Maruyama T, Romano M, Zaina F. Braces for idiopathic scoliosis in adolescents. Cochrane Database Syst Rev 2015;18(6): CD006850. doi: 10.1002/14651858.CD006850.pub3.

Newton P, Khandwala Y, Bartley C, Reighard F, Bastrom T, Yaszay B. New EOS imaging protocol allows a substantial reduction in radiation exposure for scoliosis patients. Spine Deform 2016;4: 138–144.

Ronckers CM, Land CE, Miller JS, Stovall M, Lonstein JE, Doody MM. Cancer mortality among women frequently exposed to radiographic examinations for spinal disorders. Radiat Res 2010;174:83–90.

Stokes IA, Bigalow LC, Moreland MS. Three-dimensional spinal curvature in idiopathic scoliosis. J Orthop Res 1987;5:102–113.

Ungi T, King F, Kempston M, Keri Z, Lasso A, Mousavi P, Rudan J, Borschneck DP, Fichtinger G. Spinal curvature measurement by tracked ultrasound snapshots. Ultrasound Med Biol 2014;40: 447–454.

Weinstein SL, Dolan LA, Wright JG, Dobbs MB. Effects of bracing in adolescents with idiopathic scoliosis. N Engl J Med 2013;369:1512–1521.

Zheng R, Hedden D, Moreau M, Southon S, Lou E, Hill D. Assessment of curve progression on children with idiopathic scoliosis using ultrasound imaging method. Eur Spine J 2018;27:2114–2119.

Zheng R, Hill D, Hedden D, Mahood J, Moreau M, Southon S, Lou E. Factors influencing spinal curvature measurements on ultrasound images for children with adolescent idiopathic scoliosis (AIS). PLoS One 2018;13 e0198792.

Zheng YP, Lee TT, Lai KK, Yip BH, Zhou GQ, Jiang WW, Cheung JC, Wong MS, Ng BK, Cheng JC, Lam TP. A reliability and validity study for Scolioscan: A radiation-free scoliosis assessment system using 3 D ultrasound imaging. Scoliosis Spinal Disord 2016;11:13.

Zhou G, Jiang W, Lai K, Zheng Y. Automatic measurement of spine curvature on 3-D ultrasound volume projection image with phase features. IEEE Trans Med Imaging 2017;36:1250–1262.